

Investigation of Self-Interaction Corrections for an Exactly Solvable Model System: Orbital Dependence and Electron Localization

Daniel Vieira and K. Capelle*

*Centro de Ciências Naturais e Humanas, Universidade Federal do ABC, Santo André,
09210-170 São Paulo, Brazil*

Received June 25, 2010

Abstract: A systematic investigation of two approximate self-interaction corrections (SICs), Perdew–Zunger SIC and Lundin–Eriksson SIC, and the local-density approximation (LDA) is performed for a model Hamiltonian whose exact many-body solution and exact LDA are known. Both SICs as well as LDA are applied in the calculation of ground-state energies, ground-state densities, energy gaps, and impurity densities of one-dimensional Hubbard chains differing in size, particle number, and interaction strength. The orbital-dependent potentials arising from either SIC are treated within the optimized-effective potential method, which we reformulate for the Hubbard model. The delocalization tendency of LDA is confronted with the localization tendency of SIC. A statistical analysis of the resulting data set sheds light on the role of SIC for weakly and strongly interacting particles and allows one to assess the performance of each methodology.

1. Introduction

Density-functional theory (DFT)^{1–3} is advancing at a rapid pace, driven by the demand of ever more accurate electronic-structure calculations. To meet this demand, ever more sophisticated density functionals are being constructed. A simultaneous, and often contradictory, demand is the applicability to larger and more complex systems, met by computational and methodological advances in the implementation of density functionals. In this context, the test, comparison, and implementation of different approximate density functionals in well-controlled environments is of crucial importance. This Article provides such a comparison for the case of orbital-dependent self-interaction corrections (SICs), using as theoretical laboratory an exactly solvable model system whose exact many-body ground-state energy and density are known, the one-dimensional Hubbard model.^{4,5} This model is known to display a crossover from weak to strong interactions, accompanied by increasing electron localization.^{6,7} We here specifically investigate the role self-interaction corrections play on each side of this crossover.

This Article is organized as follows: In section 2.1, we describe two different self-interaction corrections, Perdew–Zunger SIC and Lundin–Eriksson SIC. In section 2.2, we introduce the one-dimensional Hubbard model, and in section 2.3 we discuss the implementation of the orbital-dependent self-interaction corrected functionals by means of the optimized-effective potential (OEP) method for the Hubbard model. In section 3, we report results from a statistical analysis of hundreds of calculations of ground-state energies, ground-state densities, energy gaps, and impurity-site densities, always in comparison with the exact results for the many-body Hamiltonian. Section 4 contains our conclusions.

2. Background

2.1. Self-Interaction Error and Self-Interaction Corrections. One electron does not interact with itself. Simple as it is, this fact is at the heart of much trouble in many-body and electronic-structure theory. Traditional density functionals, such as the local density approximation (LDA), local spin-density approximation (LSDA), and generalized-gradient approximations (GGAs), as well as many more recently developed functionals, such as hybrids and meta GGAs, do have a spurious self-interaction error

* Corresponding author e-mail: klaus.capelle@ufabc.edu.br.

(SIE), and as a consequence predict a nonzero interaction energy even for a single electron.⁸ Consequences of the SIE of approximate functionals are multifarious and include wrong asymptotics of approximate exchange-correlation (XC) potentials, energy gaps, ionization energies, electron affinities, and transition-metal magnetic moments.

A very successful proposal for a self-interaction correction, made in 1981 by Perdew and Zunger (PZ),⁹ is

$$E_{xc}^{PZSIC}[n_\uparrow, n_\downarrow] = E_{xc}^{approx}[n_\uparrow, n_\downarrow] - \sum_k^{occ} \sum_{\sigma=\uparrow, \downarrow} (E_H[n_{k\sigma}] + E_{xc}^{approx}[n_{k\sigma}, 0]) \quad (1)$$

where $n_\sigma(\mathbf{r}) = \sum_k^{occ} n_{k\sigma}(\mathbf{r})$, $n_{k\sigma}(\mathbf{r}) = |\varphi_{k\sigma}(\mathbf{r})|^2$, and $\varphi_{k\sigma}(\mathbf{r})$ are single-particle orbitals. In PZSIC, the SIE is subtracted on a orbital by orbital basis. Evidently, for a one-electron density $E_{xc}^{PZSIC}[n^{(1)}] = -E_H[n^{(1)}]$, so that the one-electron SIE (1-SIE) is completely removed from the energy functional.

The PZSIC functional depends explicitly on the partial (orbital) densities $n_{k\sigma}(\mathbf{r})$ and, through these, on the orbitals $\varphi_{k\sigma}(\mathbf{r})$. Therefore, its minimization with respect to $n_\sigma(\mathbf{r})$ must employ the optimized-effective potential (OEP) method or one of its simplifications.^{10–14} In practice, however, the functional is usually minimized only with respect to the orbital densities $n_{k\sigma}(\mathbf{r})$, because the derivative of the PZ energy functional with respect to $n_{k\sigma}(\mathbf{r})$ can be calculated directly. The resulting orbital-specific (i.e., k -dependent) effective single-particle potential is

$$v_{s,k\sigma}^{PZSIC}(\mathbf{r}) = v_{ext}(\mathbf{r}) + v_H[n](\mathbf{r}) + v_{xc,\sigma}^{approx}[n_\sigma, n_{\bar{\sigma}}](\mathbf{r}) - v_H[n_{k\sigma}](\mathbf{r}) - v_{xc,\sigma}^{approx}[n_{k\sigma}, 0](\mathbf{r}) \quad (2)$$

$$=: v_{ext}(\mathbf{r}) + v_H[n](\mathbf{r}) + v_{xc,k\sigma}^{PZSIC}[n_\sigma, n_{\bar{\sigma}}](\mathbf{r}) \quad (3)$$

We note that this potential depends on the orbital it acts on, but is constructed from the density of all orbitals. The PZSIC approach, simplified by minimizing with respect to orbital densities instead of the spin densities, has been very successful in removing the one-electron SIE in solids.¹⁵ Results from proper minimization with respect to the densities, by means of the OEP, have also been reported for atomic^{16,17} and molecular systems.^{18–22} PZSIC has become so popular that frequently the abbreviation SIC is used as synonymous with PZSIC, but it has been repeatedly noted that the PZ proposal is not the only possibility for removing the SIE.^{23–27}

An innovative proposal for an alternative self-interaction correction was put forward in 2001 by Lundin and Eriksson (LE).²⁷ The LE proposal attempts to construct an effective potential that, when acting on the orbital of one electron, is constructed only from the density of the other orbitals. In practice, this is done by introducing an orbital-specific effective potential that is determined by subtracting from the full density $n(\mathbf{r})$ the partial density of the orbital the potential acts on:^{27–29}

$$v_{s,k\sigma}^{LESIC}(\mathbf{r}) = v_{ext}(\mathbf{r}) + v_H[n - n_{k\sigma}](\mathbf{r}) + v_{xc}^{approx}[n_\sigma - n_{k\sigma}, n_{\bar{\sigma}}](\mathbf{r}) \quad (4)$$

$$= v_{ext}(\mathbf{r}) + v_H[n](\mathbf{r}) - v_H[n_{k\sigma}](\mathbf{r}) + v_{xc}^{approx}[n_\sigma - n_{k\sigma}, n_{\bar{\sigma}}](\mathbf{r}) \quad (5)$$

$$=: v_{ext}(\mathbf{r}) + v_H[n](\mathbf{r}) + v_{xc,k\sigma}^{LESIC}[n_\sigma, n_{\bar{\sigma}}](\mathbf{r}) \quad (6)$$

where the step from eq 4 to eq 5 exploits the linearity of the Hartree potential, and eq 6 is the definition of $v_{xc,k\sigma}^{LESIC}$. In this way, the approximate effective potential acting on a given orbital, $v_{s,k\sigma}^{LESIC}(\mathbf{r})$, is constructed only from the density arising from the other orbitals. Clearly, for a one-particle system, this approach also correctly zeroes the one-electron SIE (1-SIE) contribution to the effective potential.

The LE proposal for a corrected effective potential is accompanied by a similar expression for the exchange-correlation energy:^{27,30}

$$E_{xc}^{LESIC}[n_\uparrow, n_\downarrow] = - \sum_k^{occ} \sum_{\sigma=\uparrow, \downarrow} E_H[n_{k\sigma}] + \sum_k^{occ} \sum_{\sigma=\uparrow, \downarrow} \int d\mathbf{r}^3 n_{k\sigma}(\mathbf{r}) e_{xc}^{approx}[n_\sigma - n_{k\sigma}, n_{\bar{\sigma}}](\mathbf{r}) \quad (7)$$

We note in passing that the change from LESIC to PZSIC can be affected by substituting

$$e_{xc}^{approx}[n_\sigma - n_{k\sigma}, n_{\bar{\sigma}}] \rightarrow e_{xc}^{approx}[n_\sigma, n_{\bar{\sigma}}] - e_{xc}^{approx}[n_{k\sigma}, 0] \quad (8)$$

and

$$v_{xc}^{approx}[n_\sigma - n_{k\sigma}, n_{\bar{\sigma}}] \rightarrow v_{xc,\sigma}^{approx}[n_\sigma, n_{\bar{\sigma}}] - v_{xc,\sigma}^{approx}[n_{k\sigma}, 0] \quad (9)$$

in the XC energy density and potential of former. For the Hartree potential, the substitution $v_H[n - n_{k\sigma}] \rightarrow v_H[n] - v_H[n_{k\sigma}]$ is an identity.

In the original LE work,²⁷ it was argued that the LE approach should be superior to the PZ approach because it removes the SIE of the potential, which, according to the original work, remains in the PZ approach. It has been objected³¹ that the LE proposal cannot be right because it would even correct the hypothetical exact functional, for which the PZ approach correctly reduces to zero. While we agree with this objection as a matter of principle, we feel that in practice the key issue is not only what the correction does to the hypothetical exact functional, but also what it does to the actually available approximate functionals. If such functionals were consistently improved by a correction, few workers would refrain from using this correction in practice, only because it overcorrects the hypothetical exact functional.

Interestingly, there are hints in the literature that approximate XC functionals do indeed benefit more from LESIC than from PZSIC. Novak et al.²⁸ compare the performance of LSDA, LSDA+PZSIC, and LSDA+LESIC in the calculation of hyperfine parameters and find that LESIC significantly improves agreement with experiment, relative to PZSIC. (Terra et al.²⁹ also reported a successful application of LESIC to hyperfine parameters.) In a separate

study, Friis et al.³² compared density distributions predicted for the Mg crystal with experimental electron diffraction data and observed that LESIC produces better core and valence densities than PZSIC.

The available data are too limited, however, to already conclude that LESIC is definitely superior, in practice, to PZSIC, in particular because, as a matter of principle, LESIC cannot be correct. It therefore becomes an important task to systematically investigate the performance of both approaches. This Article is a first step toward this task, providing a systematic analysis of the performance of PZSIC, LESIC, and LDA in a well-controlled model system whose exact solution is known, the one-dimensional Hubbard model.

2.2. The Hubbard Model. The Hubbard model^{4,5} (HM) is one of the most important models in quantum mechanics. In one dimension, and in second-quantized notation, the HM is defined as

$$\hat{H} = -t \sum_{i,\sigma}^L (c_{i\sigma}^\dagger c_{i+1,\sigma} + \text{H.c.}) + U \sum_i^L c_{i\uparrow}^\dagger c_{i\downarrow}^\dagger c_{i\downarrow} c_{i\uparrow} + \sum_{i,\sigma}^L V_i c_{i\sigma}^\dagger c_{i\sigma} \quad (10)$$

where L is the number of sites, t represents the amplitude for hopping between neighboring sites, U is the local (on-site) interaction, and V_i is a local external potential acting on site i . Frequently, V_i is taken to be zero, but here we include this term explicitly to describe spatial inhomogeneities, such as impurities. Occupation of each site is limited to two particles, necessarily of opposite spin. Like-spin particles do not interact in the most common form of the model. The HM is a minimal model accounting for the competition between itineracy and localization of electrons. While it is widely used in solid-state physics to describe metallic and insulating phases of correlated solids, it may also be considered a special case of the PPP model occasionally used in quantum chemistry.³³

The basic Hohenberg–Kohn and Kohn–Sham theorems of DFT hold for the HM too, once the density $n(\mathbf{r})$ is replaced by the on-site occupation number.^{34,35}

$$n(\mathbf{r}) = \sum_{\sigma} n_{\sigma}(\mathbf{r}) \rightarrow n(i) = \sum_{\sigma} n_{\sigma}(i) = \sum_{\sigma} \langle c_{i\sigma}^\dagger c_{i\sigma} \rangle \quad (11)$$

In terms of this variable, local-density and spin-density approximations for Hubbard chains and rings have been constructed^{36–38} and can be employed in the usual way.

What makes this model attractive as a theoretical laboratory for DFT is that its exact many-body solution is known in the thermodynamic limit ($L \rightarrow \infty$, $n(i) = n = N/L = \text{const}$),³⁹ and an exact numerical solution is possible for small systems (up to $L \approx 14$ on a workstation, for arbitrary density distributions $n(i)$). As a consequence of the availability of the exact solution for the infinite homogeneous system, the exact LDA is known too.⁴⁰ Moreover, a complete basis consists of two spin–orbitals per site, so that we can always work at the basis-set limit. Another welcome feature, which we will exploit below, is that the model allows one to continuously vary the interaction strength both in the exact and in the DFT calculations, which simulates the behavior

of weakly and strongly interacting systems in ab initio calculations.

We stress that the Hubbard model, when used in this spirit, is a theoretical laboratory for many-body quantum mechanics, not a simplified description of a real system. In particular, the values of U and E and the corresponding wave functions need not be derived from the Wannier orbitals obtained from an ab initio calculation of a real system.

2.3. Optimized Effective Potential Method. Formally, the local orbital-independent XC potential corresponding to a given approximation to $E_{xc}[n_{\sigma}, n_{\bar{\sigma}}]$ is given by

$$v_{xc,\sigma}^{\text{approx}}[n_{\sigma}, n_{\bar{\sigma}}](i) = \frac{\delta E_{xc}^{\text{approx}}[n_{\sigma}, n_{\bar{\sigma}}]}{\delta n_{\sigma}(i)} \quad (12)$$

where the continuous spatial argument (\mathbf{r}) from section 2.1 has been replaced by the discrete site label i .

For orbital-dependent functionals $E_{xc}^{\text{orb}}[\{\varphi_{k\sigma}\}]$, a common multiplicative potential for all orbitals can be generated by means of the OEP method,¹⁰ whose equation for discrete Hubbard chains reads

$$v_{xc,\sigma}^{\text{OEP}}[n_{\sigma}, n_{\bar{\sigma}}](i) = \frac{1}{2n_{\sigma}(i)} \sum_k^{N_{\sigma}} \{n_{k\sigma}(i)[v_{xc,k\sigma}[n_{\sigma}, n_{\bar{\sigma}}](i) + \bar{v}_{xc,k\sigma}^{\text{OEP}}[n_{\sigma}, n_{\bar{\sigma}}] - \varphi_{k\sigma}(i)\hat{t}_s\Delta_{k\sigma}^*(i) + \Delta_{k\sigma}^*(i)\hat{t}_s\varphi_{k\sigma}(i)\} + \text{c.c.} \quad (13)$$

where

$$\Delta_{k\sigma}^*(i) = - \sum_{m(m \neq k)}^L \frac{\varphi_{m\sigma}^*(i)}{\varepsilon_{k\sigma} - \varepsilon_{m\sigma}} \sum_{j=1}^L \varphi_{k\sigma}^*(j)[v_{xc,k\sigma}[n_{\sigma}, n_{\bar{\sigma}}](j) - v_{xc,\sigma}^{\text{OEP}}[n_{\sigma}, n_{\bar{\sigma}}](j)]\varphi_{m\sigma}(j) \quad (14)$$

and the barred quantities are defined as

$$\bar{v}_{xc,k\sigma}^{\text{OEP}}[n_{\sigma}, n_{\bar{\sigma}}] = \sum_{i=1}^L n_{k\sigma}(i)v_{xc,\sigma}^{\text{OEP}}[n_{\sigma}, n_{\bar{\sigma}}](i) \quad (15)$$

and

$$\bar{v}_{xc,k\sigma}[n_{\sigma}, n_{\bar{\sigma}}] = \sum_{i=1}^L n_{k\sigma}(i)v_{xc,k\sigma}[n_{\sigma}, n_{\bar{\sigma}}](i) \quad (16)$$

The terms \hat{t}_s , $\varepsilon_{k\sigma}$, and $\varphi_{k\sigma}(i)$ stand for the single-particle kinetic energy operator and the OEP-type Kohn–Sham (KS) eigenvalues and orbitals, respectively.

The preceding equation can be applied directly to the PZSIC functional to generate the corresponding KS potential. In the case of the LESIC functional, however, an additional ambiguity arises, because the LE energy expression (7) is constructed in analogy to eq 6, but its functional derivative with respect to either $n_{\sigma}(\mathbf{r})$ or $n_{k\sigma}(\mathbf{r})$ is not the LE XC potential in eq 6. Rather, the LE energy and potential are separate constructions.

Consequently, there are (at least) two possibilities to construct a local multiplicative Kohn–Sham potential for the LE approach. One is to apply the OEP to the orbital-dependent LE energy functional (7), in complete analogy to

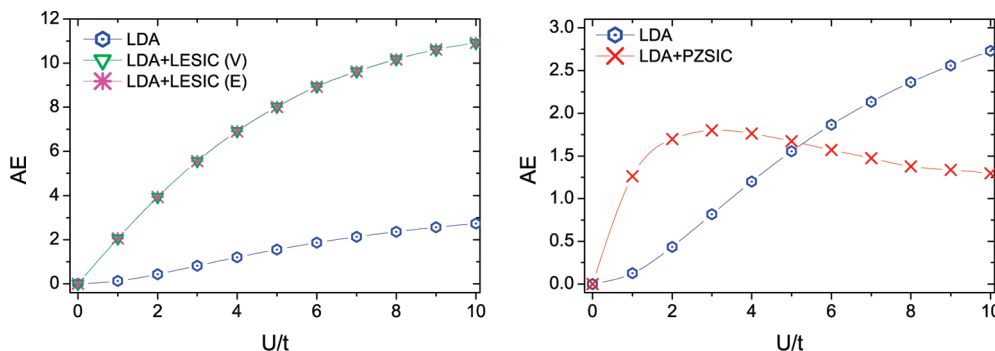


Figure 1. Average error in the ground-state energy, as defined in eq 17, for LDA and for LDA corrected by the Lundin–Eriksson (in its two flavors, V and E) and Perdew–Zunger self-interaction corrections, relative to the exact many-body ground-state energy. $N_S = 37$ systems are considered at each U/t .

what is done for the PZ energy functional (1). This requires differentiating the LE energy functional with respect to the partial densities to generate the corresponding orbital-dependent potential. We refer to this approach as LESIC(E) to emphasize that it makes use of the LE proposal for the energy and derives the XC potential from that.

Alternatively, we can formally introduce a second, hypothetical, LE energy functional, say $E_{xc}^{LESIC-h}[n_\sigma, n_{\bar{\sigma}}]$, such that its derivative with respect to the partial densities is the LE potential (6). In practice, this hypothetical energy functional need not be known explicitly, because all that is required to solve the KS equation is to substitute the orbital-specific potential (6) in the OEP equation to generate a common KS potential for all orbitals. This is the prescription followed, for example, in the study of discontinuities of the time-dependent XC potential via SIC calculations.⁴¹ Once the KS orbitals and densities have been obtained, we then follow the original LE proposal and calculate the energy correction from eq 7. This implementation is referred to as LESIC(V), to emphasize that it makes use of the LE proposal directly for the potential.

Either procedure formally eliminates the key feature of the LE correction that the potential acting on a given orbital is constructed only from the density of the other orbitals, because by construction the OEP delivers a common multiplicative potential for all orbitals. However, the feature is implicitly preserved by the OEP, because the resulting Kohn–Sham potential self-consistently produces the orbitals and densities that minimize the LE energy E_{xc}^{LESIC} or $E_{xc}^{LESIC-h}$, respectively.

3. Results

In this section, we compare the two self-interaction corrections LDA+PZSIC and LDA+LESIC (in its two flavors E and V), and the uncorrected LDA functional, using the OEP method of eq 13 to deal with the orbital-specific PZ and LE potentials. All calculations are done for finite chains of different lengths L , particle numbers N , and interaction strengths U . Variation of these parameters for each combination of methodology produces thousands of data, which we analyze statistically by reporting average errors, specifically defined for each observable. These observables are the ground-state energies (section 3.1), ground-state densities

Table 1. Average Error in the Ground-State Energy, As Defined in Eq 17, Separately for Weakly and for Strongly Interacting Systems (Columns 1 and 2) and for All Investigated Systems (Column 3)^a

N_S :	$U/t = 1...5$	$U/t = 6...10$	$U/t = 1...10$
	185	259	444
LDA	0.8264	2.3301	1.5782
LDA+LESIC(V)	5.3011	10.0576	7.6794
LDA+LESIC(E)	5.2954	10.0508	7.6731
LDA+PZSIC	1.6388	1.4104	1.5246

^a Entries in boldface are the best in each column (interaction regime).

(section 3.2), energy gaps (section 3.3), and impurity-site densities (section 4).

3.1. Ground-State Energies. We start by evaluating the total ground-state energy. For each data set (see below), the accumulated deviation between approximate and exact results is measured by means of the percentage average error defined as

$$AE = 100 \frac{\sum_{j=1}^{N_S} |E_{\text{approx}}^j - E_{\text{exact}}^j|}{\sum_{j=1}^{N_S} |E_{\text{exact}}^j|} \quad (17)$$

where E_{exact}^j refers to numerically exact many-body energies for the same set of model parameters. N_S is the number of systems in the data set.

Our results are summarized in Figure 1 and Table 1. The figure compares the average error defined in eq 17 as a function of interaction strength U , ranging from the noninteracting system $U = 0$, over weakly $U \approx 2t$, moderately $U \approx 6t$, to strongly $U \approx 10t$ interacting systems. For each value of U , our sample consists of $N_S = 37$ chains of different sizes, particle number, and densities ($L = 3, 4, 5, \dots, 14$ and $N = 2, 4, 6, \dots, 10$, with $N/L < 0.85$). All systems have $V_i = 0$ (no impurities) but are spatially inhomogeneous due to the density modulations arising due to the boundaries.

First, comparing both SICs, we find that LDA+PZSIC consistently performs better than LDA+LESIC(V) and LDA+LESIC(E). To permit a better visualization, the scale on the vertical axis of the two figures is not the same, but the values of the average error are directly comparable and

leave little doubt about the superiority of PZSIC energies for these systems.

Next, we note that for weakly interacting systems (where the physics is dominated by the kinetic energy term, and the particles are delocalized), LDA alone is actually better than LDA+PZSIC and LDA+LESIC. Of course, both SICs remove the self-interaction error of the LDA also in this regime, but they are not exact themselves, and thus introduce other errors. For weak interactions, it does not pay to correct a small error by a correction introducing larger ones. For stronger interactions, the particles start to localize, the SIE becomes more important, and its removal by PZSIC improves the total energies considerably. The crossover between the error curves occurs around $U \approx 5t$. The separation in these two regimes is a rather gratifying result to obtain, as $U \approx 5t$ is known to mark the region where the Hubbard model crosses over from weakly to strongly interacting systems, and the electrons become increasingly localized.^{6,7} The performance of PZSIC is clearly related to this crossover, which is a signature of strong correlation. In fact, in retrospect, one could have predicted that the electrons in the Hubbard model start to localize around $U \approx 5t$ simply by comparing the relative performance of LDA and LDA+PZSIC as a function of U .

In this context, numerical evidence of electronic localization is obtained by calculation of the double occupation (D) factor, which, for any system j , is defined as the expectation value of the interaction energy divided by U :

$$D_j = \sum_{i=1}^{L_j} \langle c_{it}^\dagger c_{it}^\dagger c_{it}^\dagger c_{it} \rangle = \frac{\partial E_{\text{approx}}^j}{\partial U} \quad (18)$$

where the second equality arises from the Hellman–Feynman theorem. In general, D_j measures the probability of a site to be doubly occupied as a function of U . For up to half-filled bands and any repulsive U , a ground-state $D > 0$ indicates that the particles are spread over various sites. Under these circumstances, D approaches zero as $U/t \rightarrow \infty$, indicating maximum localization. Considering our previous sample of $N_s = 37$ systems, we evaluate the average value of D_j :

$$AD = \frac{\sum_{j=1}^{N_s} D_j}{\sum_{j=1}^{N_s} 1} \quad (19)$$

Results are summarized in Figure 2.

First, the comparison of both SICs indicates that LESIC (in its two flavors) tends to overlocalize the electrons, reducing the average value of D . This trend to localize strongly agrees with similar observations in the original LE work.²⁷ The LDA functional, on the other hand, tends to enforce double occupation and delocalize the electrons, resulting in more accurate results for weak interactions. By contrast, the LDA+PZSIC approach overlocalizes particles up to $U \approx 3t$. For stronger values of U , the LDA+PZSIC functional crosses the exact curve and becomes superior to LDA, yielding localized states whose double occupation

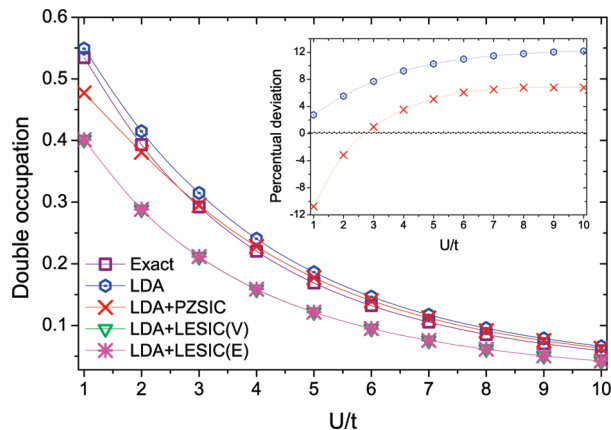


Figure 2. Average double occupation, as defined in eq 19, for exact diagonalization, LDA, and for LDA corrected by LESIC and PZSIC. $N_s = 37$ systems are considered at each U/t . Inset: Average percentual deviations with respect to the exact data.

curve is closer to the exact one. These conclusions are reinforced by the inset, which compares the percentual deviations of LDA and LDA+PZSIC. We note that localization is mainly driven by the onsite interaction, with electrons behaving like noninteracting spinless fermions as $U/t \rightarrow \infty$. The transition from LDA to LDA+PZSIC further localizes the electrons, reducing the spurious self-interaction, which favors delocalization.

To make this division in two distinct regimes clearer, we report in Table 1 the average error for each regime, that is, sum not only over systems with different size and particle number, but also over those with interaction strengths in the indicated range. The lowest average error in each regime is printed in boldface. Clearly, for weakly interacting systems, LDA does best. For strongly interacting systems, on the other hand, LDA+PZSIC wins. Overall, that is, considering the average error over all considered systems regardless of the value of U , LDA+PZSIC is the best combination among all methodologies tested here. Turning to a comparison of the different flavors of LESIC among each other, we note that the LDA+LESIC(E) and LDA+LESIC(V) approaches, despite their different starting points, give very similar results.

3.2. Ground-State Densities. Next, we turn to ground-state densities. To quantify the average error of these quantities, we sum for each system (labeled by j) and for all sites (labeled by i) the local absolute deviation between exact and approximate densities and express the resulting error as

$$AEn = 100 \frac{\sum_{j=1}^{N_s} \sum_{i=1}^{L_j} |n_{\text{approx}}^j(i) - n_{\text{exact}}^j(i)|}{\sum_{j=1}^{N_s} \sum_{i=1}^{L_j} |n_{\text{exact}}^j(i)|} \quad (20)$$

where L_j labels the total number of sites i composing each system j . Considering the same set of systems that we have considered for the total ground-state energies, the results for the average error in the ground-state densities are summarized in Figure 3 and in Table 2.

From Figure 3a we first note that uncorrected LDA performs better than any of the SICs and that LDA+PZSIC

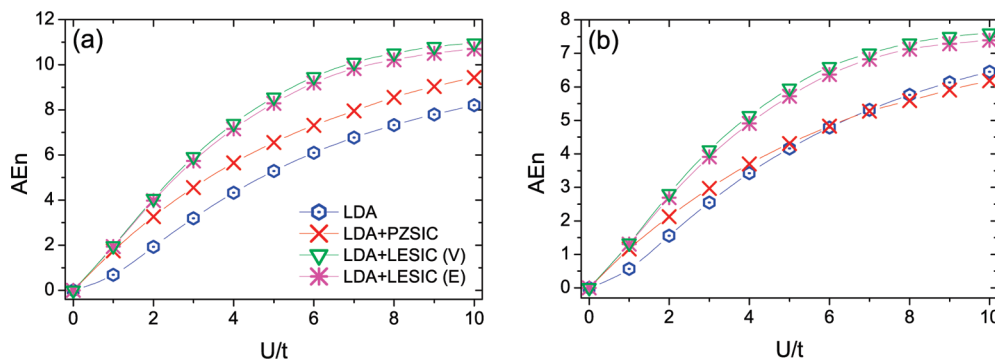


Figure 3. Average error in the ground-state density, as defined in eq 20, for LDA and for LDA corrected by LESIC and PZSIC, relative to the exact many-body ground-state density. (a) $N_S = 37$ systems are considered at each U/t ; (b) $N_S = 17$ systems are considered at each U/t .

Table 2. Average Error in the Ground-State Density, As Defined in Eq 20, Separately for Weakly and for Strongly Interacting Systems (Columns 1 and 2) and Jointly for All Investigated Systems (Column 3)^a

	$U/t = 1...5$	$U/t = 6...10$	$U/t = 1...10$
N_S :	185	259	444
LDA	3.0830	7.2373	5.1602
LDA+LESIC(V)	5.5745	10.36087	7.9676
LDA+LESIC(E)	5.4191	10.0873	7.7532
LDA+PZSIC	4.3526	8.4551	6.40381
N_S :	80	112	192
LDA	2.4536	5.6875	4.0706
LDA+LESIC(V)	3.8683	7.1997	5.5340
LDA+LESIC(E)	3.7070	6.9978	5.3524
LDA+PZSIC	2.8523	5.5571	4.2047

^a Entries in boldface are the best in each column. First group of data: complete statistics, including all sites. Second group of data: reduced statistics after exclusion of the border and central sites.

is better than LDA+LESIC(E) and LDA+LESIC(V). The relation between the various curves is rather different from what it was for the energies; in particular, there is no crossover between LDA and LDA+PZSIC.

Upon closer investigation of the exact and approximate density profiles, one finds that the LDA densities are closer to the exact ones than the SIC ones mostly at the borders of the chains, where the densities are reduced due to the presence of the boundary, and consequently the SIE is reduced too. At the central site (of systems with odd number of sites L , where a central site is well-defined), the SIC density is also substantially worse than the LDA one. Therefore, we additionally calculated the average errors after eliminating the boundary sites, as well as the central one. The result is shown in Figure 3b and clearly displays a crossover between LDA and LDA+PZSIC for sufficiently large values of U , just as was found for the total energies. We conclude that PZSIC densities are worse at the surface of the systems and at their geometric center, but that this local behavior has little effect on the global energies, which are dominated by the other sites.

For LDA+LESIC(V) and LDA+LESIC(E), on the other hand, even exclusion of these critical sites has no beneficial effect, and both continue to perform worse than uncorrected LDA for all U . We believe that this is an intrinsic problem of the LESIC (not due to the OEP-like implementation), because it is reproduced also in other implementations: in

unpublished calculations, we implemented LESIC via the GAM, Slater, and KLI approximations to the OEP equation,¹⁰ as well as through globally and locally scaled self-consistency.⁴² The behavior of LESIC is consistently worse than that of PZSIC, in any of these different modes of implementation. The same applies even for post-LDA calculations of total energies. The explanation is probably that LESIC overcorrects the LDA functional in the sense that it would even “correct” the exact functional.

Table 2 summarizes these discussions by displaying the average error separately for weak and strong interaction, as well as for all interactions, with and without elimination of boundary and central sites.

3.3. Energy Gaps. Besides the ground-state energy itself, the calculation of energy differences is also of interest because there is no guarantee that the trends we identified for energies will survive cancellation upon forming the difference. For this reason, we also evaluate the fundamental energy gap, defined as

$$E_g = E(N-1, L) - E(N, L) - [E(N, L) - E(N+1, L)] \quad (21)$$

where $E(N, L)$ labels the ground-state energy of a N electron system with L sites. Our data set comprises systems with $L = 4, 6, 7, \dots, 14$ sites, which for $N = 2, 4, 6, 8, 10$ (with $N/L < 0.85$) displays a band gap due to the system boundary, and for $U > 0$ and $N/L = 1.0$ with periodic boundary conditions (so that $n = 1$ on all sites) features a Mott gap. Previous work³⁷ already demonstrated that the Bethe–Ansatz LDA functional we use for the Hubbard model properly accounts for the Mott gap in homogeneous systems and provides a reasonable approximation to it in inhomogeneous systems. Here, we inquire whether the description of inhomogeneous systems is further improved by self-interaction corrections.

Similarly to the previous cases, we measure the average error in the gap by

$$AE_g = 100 \frac{\sum_{j=1}^{N_S} |E_{g, \text{approx}}^j - E_{g, \text{exact}}^j|}{\sum_{j=1}^{N_S} |E_{g, \text{exact}}^j|} \quad (22)$$

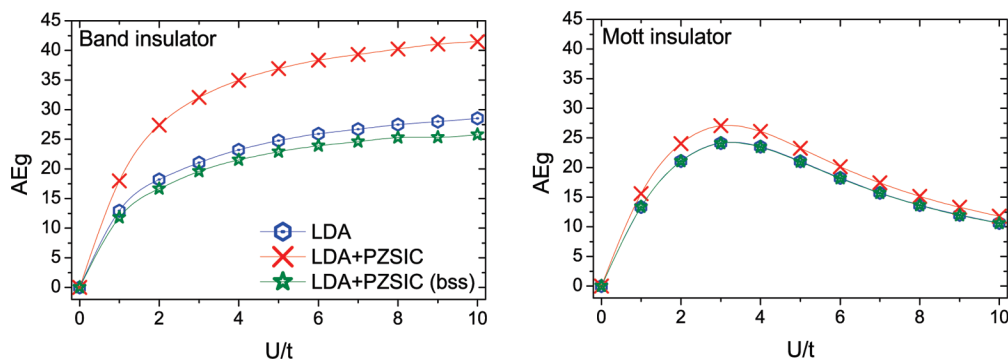


Figure 4. Average error in the energy gap, as defined in eq 22, for LDA and for LDA corrected by PZSIC (via post-LDA implementation), relative to the exact fundamental energy gap. The starred (green) data refer to calculations with broken spin symmetry (bss).

for the approximate and exact energy gap E_g^j of each system j . Results are shown in Figure 4. In this section, we employ post-LDA implementations of the SIC functionals instead of following the OEP procedure, which converges very badly when $N/L = 1.0$.

For both the band gap and the Mott gap, LDA+PZSIC is vastly superior over LDA+LESIC for all values of U . For simplicity, we therefore do not show LESIC data in the figures. Interestingly, the PZSIC results, although better than the LESIC ones, perform consistently worse than uncorrected LDA for all U . Unlike for total energies, there is no crossover between LDA and LDA+PZSIC curves even for large values of U . Because LDA+PZSIC yields the more accurate individual total energies, this improved performance for energy differences must be due to error cancellation upon subtraction, as frequently occurs within LDA.

Interestingly, comparison of both panels of Figure 4 clearly shows that the advantage LDA has over LDA+PZSIC is

much smaller for Mott insulators than for band insulators. This behavior is consistent with our previous findings, as in the Mott insulator the particles are more localized, LDA energies become worse, SIC energies become better, and the advantaged LDA derives from error cancellation is reduced.

In the LDA calculations, spin-symmetry is never broken. In the SIC calculations described so far, we explicitly enforced spin symmetry for systems with odd total particle number, by fractionally occupying the highest up and down orbitals. Alternatively, we can also permit the system to break spin symmetry, by placing the last electron completely in the highest orbital of one spin (say up). The resulting system displays an incorrect magnetization, but lower total energies and a much improved band and Mott gaps, as displayed in the starred (green) curves in Figure 4. For the band insulator, this improvement is enough to overcome the gain LDA obtained from error cancellation and transform PZSIC into the best performing functional, at the expense, however, of

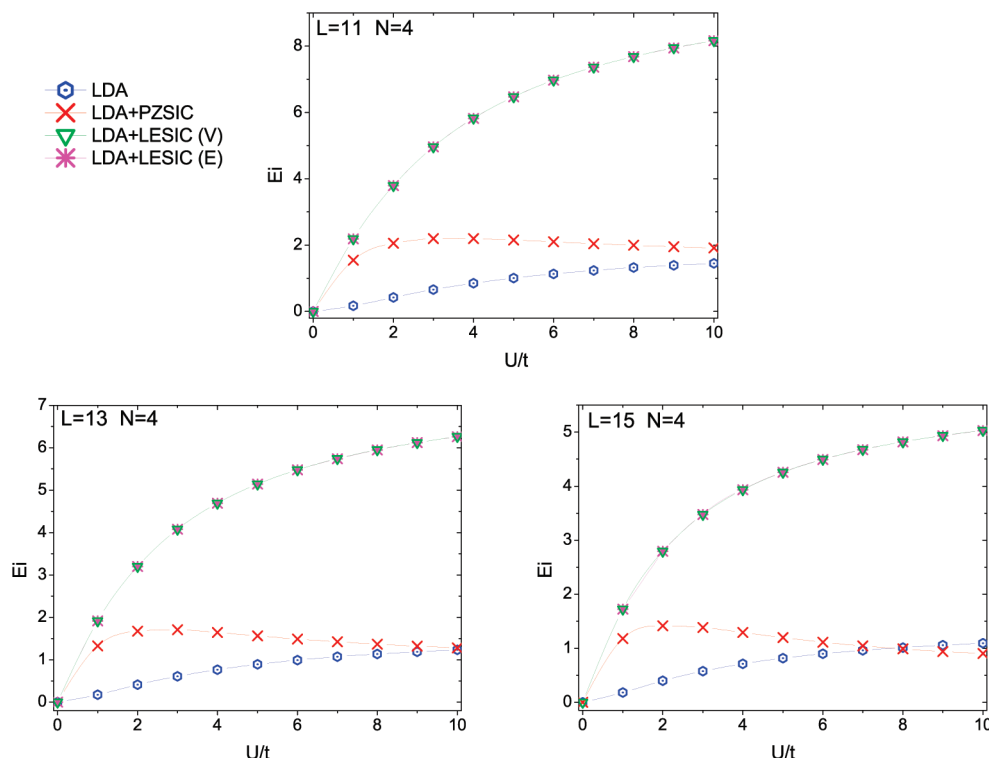


Figure 5. Error in the ground-state energy of the attractive impurity system, as defined in eq 23, relative to the exact many-body ground-state energy.

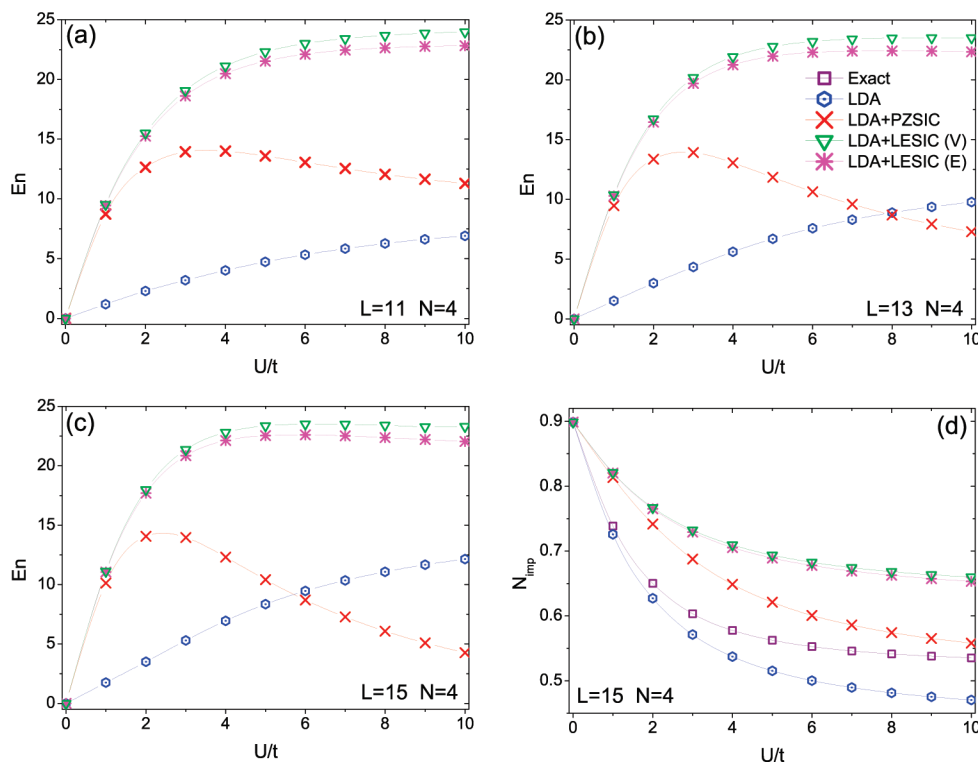


Figure 6. (a–c) Error in the ground-state density at the attractive impurity site, as defined in eq 24, relative to the exact many-body ground-state density. (d) Number of electrons N_{imp} at the impurity site.

wrong spin densities. This is the same tendency known from ab initio applications of PZSIC.⁹

3.4. Ground-State Energies and Densities in the Presence of a Local Impurity. So far, we have investigated chains without any additional external potentials. An interesting complementary analysis consists of considering systems with local impurities. Because of the very large number of possible variations of system parameters (which now include location, concentration and strength of the impurities), we here do not perform a statistical analysis, but rather a case study, limiting us to consider a few typical situations. Nevertheless, we consider different average densities N/L because the value of U that characterizes the crossover from weak to strong interactions can slightly depend on the average density.

As a function of the interaction U , the results are shown in Figures 5–8, in which we plot the percentual absolute error with respect to the exact results, defined as

$$Ei = 100 \frac{|E_{\text{approx}} - E_{\text{exact}}|}{|E_{\text{exact}}|} \quad (23)$$

for the ground-state energy and

$$En = 100 \frac{|n_{\text{approx}}(\text{imp}) - n_{\text{exact}}(\text{imp})|}{|n_{\text{exact}}(\text{imp})|} \quad (24)$$

for the density at the impurity site. As our sample, we take $N = 4$, with $L = 11, 13$, and 15 . First, we place an attractive impurity of magnitude $V_{\text{imp}} = -1.0t$ at the central site. This potential favors electron localization at the impurity site and competes with the local repulsive interaction U . In a separate

set of calculations, we consider a repulsive impurity of magnitude $V_{\text{imp}} = 1.0t$, also at the central site. Contrary to the attractive case, the repulsive impurity favors delocalization of electrons. By comparing both cases, we can thus analyze and assess the effects of the LDA and SIC on the delocalization and delocalization of electrons, respectively.

For the attractive impurity, considering either energies or densities, we see from Figures 5 and 6 a crossover between LDA and LDA+PZSIC whose precise location depends on the average density N/L . Again, no crossover is seen for LDA+LESIC(V) and LDA+LESIC(E). For our sample of systems, we find that the smaller is the average density, the smaller becomes the interaction U for which LDA+PZSIC starts to produce better results than uncorrected LDA. This is in accordance with the expectation that strong correlations are not only characterized by large values of U but also by low densities, and also with similar trends observed in calculations not using DFT.⁷

In Figure 6d, where we plot the density at the impurity site, we note the same tendency of electronic localization already seen in Figure 2: both LESIC approaches tend to strongly overlocalize electrons, PZSIC somewhat overlocalizes, while LDA overly delocalizes.

In the repulsive impurity case, depicted in Figure 7, our previous conclusions for the ground-state energies still hold. There is a clear crossover between LDA and LDA+PZSIC, which depends on the average density. On the other hand, for the densities at the impurity sites we see from Figure 8 that the uncorrected LDA surpasses all alternative approaches, for all values of U and N/L . This is because the repulsive impurity tends to delocalize the electrons, thus

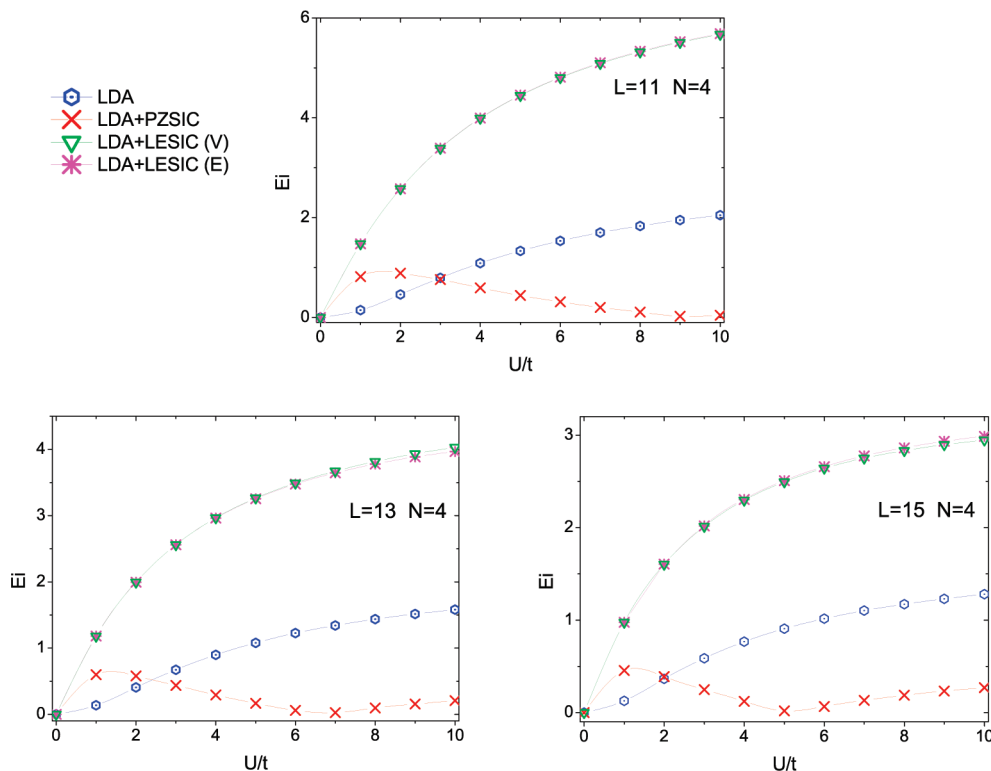


Figure 7. Error in the ground-state energy of the repulsive impurity system, as defined in eq 23, relative to the exact many-body ground-state energy.

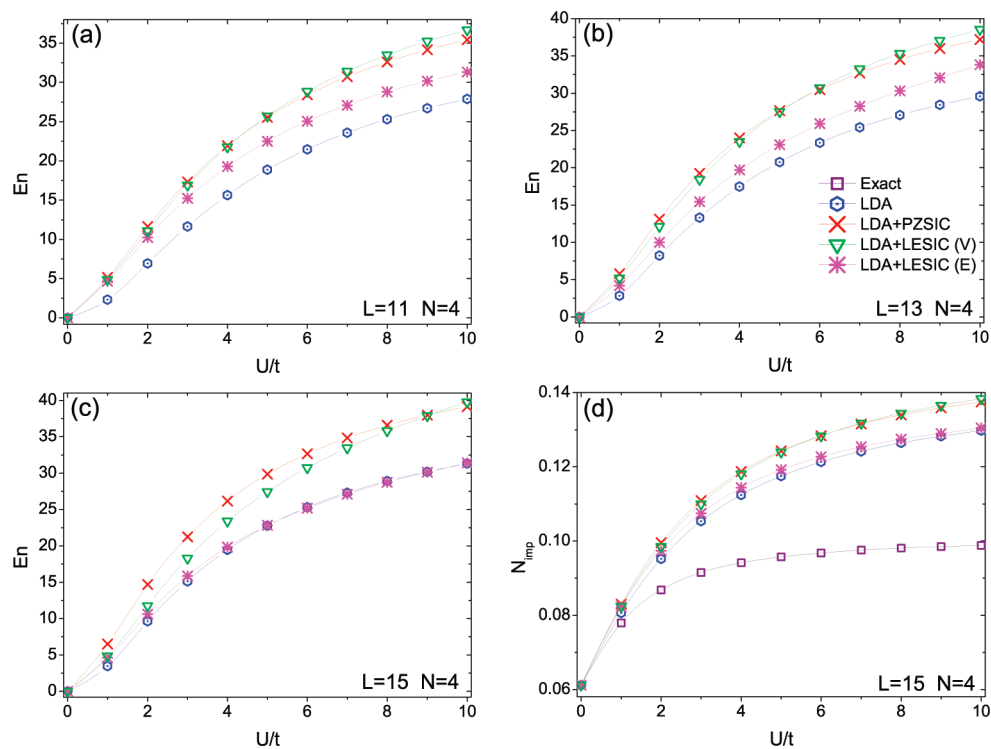


Figure 8. (a–c) Error in the ground-state density at the repulsive impurity site, as defined in eq 24, relative to the exact many-body ground-state density. (d) Number of electrons N_{imp} at the impurity site.

producing a situation in which the LDA is more reliable. Nevertheless, for ground-state energies, which are obtained from the densities of all sites of the Hubbard chain, LDA+PZSIC still delivers more accurate results in the strongly interacting regime.

4. Conclusions

We performed self-consistent calculations for the one-dimensional Hubbard model within the LDA and two orbital-dependent self-interaction corrections, in various implemen-

tations, and analyzed their performance by means of statistical comparison to the numerically exact many-body solution of the same model. Several trends emerge from this analysis:

(i) For the weakly interacting systems, the benefit of an approximate SIC is overcompensated by the intrinsic errors of the approximation. Uncorrected LDA here works best, for all investigated quantities and systems.

(ii) For more strongly interacting situations, correcting the SIE is important, but of the investigated corrections only PZSIC systematically improves on the LDA ground-state energies. Although it yields the most accurate total energies, PZSIC does not improve fundamental energy gaps, for which LDA benefits from substantial error cancellation, unless spin symmetry is allowed to break, in which case PZSIC becomes superior.

(iii) Despite their differences in the treatment of the potential, LESIC(E) and LESIC(V) produce quite similar results and are consistently worse than all other tested approaches, for energies and densities.

(iv) The crossover between the regimes where PZSIC worsens and improves on LDA is characterized by increasing localization. Its precise position as a function of interaction strength depends on the average density N/L . PZSIC turns out to be beneficial for lower densities and stronger interactions. The relative performance of LDA and LDA+PZSIC energies is found to be a clear indicator of the crossover between weak and strong correlations, and the concomitant localization, in the Hubbard model.

(v) Conclusions iii and iv also apply to ground-state densities, however, only if one ignores the densities right at the borders and at the central site of the systems, where PZSIC performs rather badly. If these sites are included, the accumulated (over all sites) error of the LDA densities is smaller than that of the LDA+PZSIC (and LDA+LESIC) densities for all investigated systems.

(vi) For impurity systems, the delocalization tendency of LDA sharply contrasts with the localization tendency of SIC. For attractive impurities, which favor electron localization, SIC performs better than LDA. On the other hand, for repulsive impurities, favoring electronic delocalization, LDA yields more accurate results than SIC. This shows that the performance of each functional is directly tied to the degree of localization, regardless of whether this localization is driven by particle–particle interactions or by external potentials.

Naturally, these conclusions may have been biased by the choice of the Hubbard model as theoretical laboratory. The disadvantages of such choice, on the other hand, are largely compensated by the availability of an exact many-body solution as a benchmark, of the exact LDA,⁴⁰ and by the absence of any problems due to finite basis sets or due to experimental uncertainties.

Other aspects of SIC, such as the asymptotic behavior of the potential of finite systems, cannot be addressed within the Hubbard model and require separate analysis. It remains to be seen if the superiority of PZSIC remains unchallenged by extension of these investigations to other corrections, implementations, and classes of systems, as well as in the study of systems of noninteger electron numbers. Similarly,

the important issue of the many-electron SIE^{43–46} requires separate investigation.

Acknowledgment. This work was supported by FAPESP and CNPq. K.C. thanks J. Terra and D. Guenzberger for bringing the LE approach to his attention. We thank V. L. Campo, Jr., for his exact diagonalization code for the Hubbard model.

References

- (1) Kohn, W. *Rev. Mod. Phys.* **1999**, 71, 1253.
- (2) Dreizler, R. M.; Gross, E. K. U. *Density Functional Theory: An Approach to the Quantum Many-Body Problem*; Springer: Berlin, Germany, 1990.
- (3) Parr, R. G.; Yang, W. *Density-Functional Theory of Atoms and Molecules*; Oxford University Press: New York, 1989.
- (4) Hubbard, J. *Proc. R. Soc. London, Ser. A* **1963**, 276, 238.
- (5) Lieb, E. H.; Wu, F. Y. *Physica A* **2003**, 321, 1.
- (6) White, S. R.; Affleck, I.; Scalapino, D. J. *Phys. Rev. B* **2002**, 65, 165122.
- (7) Bedürftig, G.; Brendel, B.; Frahm, H.; Noack, R. M. *Phys. Rev. B* **1998**, 58, 10225.
- (8) The exact exchange energy of one electron exactly cancels its Hartree energy, so that the Hartree + exchange energy of methods employing exact exchange is self-interaction free, but the correlation energy remains subject to self-interaction even in methods employing exact exchange.
- (9) Perdew, J. P.; Zunger, A. *Phys. Rev. B* **1981**, 23, 5048.
- (10) Kümmel, S.; Kronik, L. *Rev. Mod. Phys.* **2008**, 80, 3.
- (11) Yang, W.; Wu, Q. *Phys. Rev. Lett.* **2002**, 89, 143002.
- (12) Kümmel, S.; Perdew, J. P. *Phys. Rev. B* **2003**, 68, 035103.
- (13) Krieger, J. B.; Li, Y.; Iafrate, G. J. *Phys. Rev. A* **1992**, 46, 5453.
- (14) Ullrich, C. A.; Reinhard, P.-G.; Suraud, E. *Phys. Rev. A* **2000**, 62, 053202.
- (15) Svane, A.; Petit, L.; Szotek, Z.; Temmerman, W. M. *Phys. Rev. B* **2007**, 76, 115116. Lüders, M.; Ernst, A.; Dane, M.; Szotek, Z.; Svane, A.; Kodderitzsch, D.; Hergert, W.; Gyorffy, B. L.; Temmerman, W. M. *Phys. Rev. B* **2005**, 71, 205109. Petit, L.; Svane, A.; Temmerman, W. M.; Szotek, Z. *Phys. Rev. B* **2001**, 63, 165107. Strange, P.; Svane, A.; Temmerman, W. M.; Szotek, S.; Winter, H. *Nature* **1999**, 399, 756.
- (16) Chen, J.; Krieger, J. B.; Li, Y.; Iafrate, G. J. *Phys. Rev. A* **1996**, 54, 3939.
- (17) Norman, M.; Koelling, D. D. *Phys. Rev. B* **1984**, 30, 5530.
- (18) Körzdörfer, T.; Mundt, M.; Kümmel, S. *Phys. Rev. Lett.* **2008**, 100, 133004.
- (19) Garza, J.; Nichols, J. A.; Dixon, D. A. *J. Chem. Phys.* **2000**, 112, 7880.
- (20) Körzdörfer, T.; Kümmel, S.; Mundt, M. *J. Chem. Phys.* **2008**, 129, 014110.
- (21) S. Patchkovskii, S.; Autschbach, J.; Ziegler, T. *J. Chem. Phys.* **2001**, 115, 26.
- (22) Pemmaraju, C. D.; Sanvito, S.; Burke, K. *Phys. Rev. B* **2008**, 77, 121204.
- (23) Fermi, E.; Amaldi, E. *Acad. Ital. Rome* **1934**, 6, 117. Ayers, P. W.; Morrison, R. C.; Parr, R. G. *Mol. Phys.* **2005**, 103, 2061.

- (24) Cortona, P. *Phys. Rev. A* **1986**, 34, 769.
- (25) Unger, H. J. *Phys. Lett. A* **2001**, 284, 124.
- (26) Vosko, S. H.; Wilk, L. J. *Phys. B: At. Mol. Phys.* **1983**, 16, 3687.
- (27) Lundin, U.; Eriksson, O. *Int. J. Quantum Chem.* **2001**, 81, 247.
- (28) Novak, P.; Kunes, J.; Pickett, W. E.; Ku, W.; Wagner, F. R. *Phys. Rev. B* **2003**, 67, 140403.
- (29) Guenzburger, D.; Ellis, D. E.; Terra, J. *Theor. Chem. Acc.* **2005**, 113, 191.
- (30) Seo, D. K. *J. Chem. Phys.* **2006**, 125, 154105.
- (31) Perdew, J. P.; Ruzsinszky, A.; Tao, J.; Staroverov, V. N.; Scuseria, G. E.; Csonka, G. I. *J. Chem. Phys.* **2005**, 123, 062201.
- (32) Friis, J.; Maden, G. K. H.; Larsen, F. K.; Jiang, B.; Marthinsen, K.; Holmestad, R. *J. Chem. Phys.* **2003**, 119, 11359.
- (33) Pariser, R.; Parr, R. G. *J. Chem. Phys.* **1953**, 21, 767. Pople, J. A. *Trans. Faraday Soc.* **1953**, 49, 1375.
- (34) Gunnarsson, O.; Schönhammer, K. *Phys. Rev. Lett.* **1986**, 56, 1968.
- (35) Schönhammer, K.; Gunnarsson, O.; Noack, R. M. *Phys. Rev. B* **1995**, 52, 2504.
- (36) Lima, N. A.; Silva, M. F.; Oliveira, L. N.; Capelle, K. *Phys. Rev. Lett.* **2003**, 90, 146402.
- (37) Lima, N. A.; Oliveira, L. N.; Capelle, K. *Europhys. Lett.* **2002**, 60, 601.
- (38) Xianlong, G.; Polini, M.; Tosi, M. P.; Campo Jr., V. L.; Capelle, K.; Rigol, M. *Phys. Rev. B* **2006**, 73, 165120.
- (39) Lieb, E. H.; Wu, F. Y. *Phys. Rev. Lett.* **1968**, 20, 1445.
- (40) By exact LDA, we mean that there is no need for analytical interpolations such as the PZ81, VWN, or PW92 forms of the ab initio LDA, because the energy of the homogeneous reference system can be calculated numerically exactly for arbitrary densities.
- (41) Vieira, D.; Capelle, K.; Ullrich, C. A. *Phys. Chem. Chem. Phys.* **2009**, 11, 4647.
- (42) Lima, M. P.; Pedroza, L. S.; Silva, A. J. R.; Fazzio, A.; Vieira, D.; Freire, H. J. P.; Capelle, K. *J. Chem. Phys.* **2007**, 126, 144107.
- (43) Ruzsinszky, A.; Perdew, J. P.; Csonka, G. I.; Vydrov, O. A.; Scuseria, G. E. *J. Chem. Phys.* **2006**, 125, 194112.
- (44) Mori-Sánchez, P.; Cohen, A. J.; Yang, W. *J. Chem. Phys.* **2006**, 125, 201102.
- (45) Cohen, A. J.; Mori-Sánchez, P.; Yang, W. *Science* **2008**, 321, 792.
- (46) Mori-Sánchez, P.; Cohen, A. J.; Yang, W. *Phys. Rev. Lett.* **2008**, 100, 146401.

CT100352R